Proceedings of the 9th World Congress on Momentum, Heat and Mass Transfer (MHMT'24)
London, United kingdom – April 11 – 13, 2024
Paper No. ENFHT 335
DOI: 10.11159/enfht24.335

Thermal Loading Analysis of Hypersonic Flight Object with Re-Entry Trajectory by Time-Adaptive Weakly Coupled Conjugate Heat Transfer

Yi-Hsun Chen[1], Tzong-Shyng Leu[2]
Department of Aeronautics and Astronautics, National Cheng Kung University
No. 1 University Road, Tainan 701, Taiwan
linsen5106@gmail.com[1]; tsleu@mail.ncku.edu.tw[2]

Abstract **-** This study focuses on assessing the thermal loading experienced by an object re-entering from altitude 60km with hypersonic speed along a specified trajectory. Traditional approaches employ strongly coupled conjugate heat transfer to address the transient flow and heat transfer interaction, necessitating extremely small time steps in unsteady flow solvers due to hypersonic conditions. However, the computational cost becomes prohibitively high, exceeding a decade for a flight time around 100 seconds. In response, this paper introduces a novel time-adaptive weakly coupled conjugate heat transfer method. This approach determines coupling times between flow and heat transfer solvers based on changes in wall heat flux and temperature. The methodology in this paper also addresses challenges such as hypersonic flow, gas chemical reactions, aerodynamic heating, and surface ablation. The trajectory is initially established using flight dynamic theory, providing time-varying free stream conditions. Computational Fluid Dynamics (CFD) predicts flow field information including shockwaves, chemical reactions, and aerodynamic heating. Thermal loading on the wall is considered in conjunction with a Thermal Protection System (TPS), employing carbon-based materials. The model accounts for gas and surface material reactions, including ablation reactions in carbon-based materials, with surface shape changes implemented using User-Defined Function (UDF) custom code. This integrated approach not only reduces computational costs but also enables real-time monitoring of surface thermal loads and structural heat transfer variations due to time-dependent free stream conditions. At the end of the paper, a practical empirical relationship is presented, establishing a correlation between thermal loads at the stagnation point and the free stream conditions throughout the flight. The utilization of this straightforward empirical equation provides a valuable tool for designing effective thermal protection systems and optimizing trajectories in the realm of future hypersonic applications.

Keywords**:** Hypersonic flow, Re-Entry Object, Aerodynamic Heating, Ablation

1. Background

In the realm of hypersonic flying objects, including established platforms like space shuttles, re-entry capsules, and ballistic missiles, as well as emerging technologies such as hypersonic guide vehicles (HGV), the operational landscape is evolving rapidly. The pursuit of higher speeds in these vehicles introduces unprecedented aero-thermal challenges, demanding advanced solutions for the thermal protection systems (TPS). Effectively mitigating the thermal loads imposed by the high-speed flow fields has become an imperative task. In this paper, we delve into the challenges posed by hypersonic flight conditions, exploring the multifaceted dynamics between hypersonic flow fields and thermal protection materials. Traditional techniques have often relied on strongly coupled conjugate heat transfer to address the intricate transient interactions between flow and heat transfer. However, the exigencies of hypersonic conditions mandate extremely small time steps in unsteady flow solvers, resulting in computational costs that surpass a decade for trajectories lasting around 100 seconds. In response, this paper introduces an innovative time-adaptive weakly coupled conjugate heat transfer method. This novel approach determines coupling times between flow and heat transfer solvers with a proportional-integral- derivative (PID) controller based on changes in wall heat flux and wall temperature.

The current methodology in this paper also extends its capabilities to tackle the challenges inherent in hypersonic flight, including gas chemical reactions, aerodynamic heating, and surface ablation. The trajectory is established using flight dynamic theory, offering insights into time-varying free stream conditions. Computational Fluid Dynamics (CFD) is used to predict flow field information, including shock waves, chemical reactions, and aerodynamic heating. The consideration of thermal loading on the wall is seamlessly integrated with a carbon-based thermal protection material. The model accounts for reactions within the gas and surface materials, including ablation reactions in carbon-based materials, with surface shape changes implemented using User-Defined Function (UDF) custom code. This integrated approach not only significantly reduces computational costs but also enables more realistic and real-time monitoring of surface thermal loads and variations in structural heat transfer due to time-dependent free stream conditions.

In the paper's conclusion, a practical empirical relationship is presented, establishing a correlation between thermal loads at the stagnation point and the free stream conditions throughout the flight. The utilization of this straightforward empirical equation provides a valuable tool for designing effective thermal protection systems and optimizing trajectories in the realm of future hypersonic applications.

2. Research Methodology

Flight Trajectory

As the focus of the study is on the aerodynamic heating during re-entry flight trajectory, it is essential to establish the trajectory of a re-entry object to obtain free stream conditions. In the ballistic re-entry stage, the object often approaches the target at high speed without thrust and lift. Fig. 1(a) is the force diagram of the re-entry object, which includes drag (D), weight (W), and the centrifugal force (F_c), while other external forces are neglected. Applying Newton's Second Law, treating the vehicle as a single particle in motion, and solving the differential equations composed of drag, gravity and centrifugal force, as shown in Eqs.(1)~(4) (refer to [1][2]). Finally, the instantaneous altitude (H), velocity (V), attitude angle ($\emptyset$), and range (X) of the vehicle during the flight are obtained. Fig. 1(b) shows the trajectory (altitude (H) vs velocity (V)) of the hypersonic re-entry object calculated in the current study.

$$\dot{H} = -V sin\emptyset \tag{1}$$

$$m\dot{V} = -D + W sin\emptyset \tag{2}$$

$$mV\dot{\emptyset} = cos\emptyset\left(W - m\frac{V^2}{(R_e + H)}\right) \tag{3}$$

$$\dot{X} = V cos\emptyset \frac{R_e}{(R_e+H)} \tag{4}$$

where $H, V, \emptyset, X, m, D$ and W is altitude, velocity, flight path angle, range, mass, drag and weight of the hypersonic flying object, respectively.

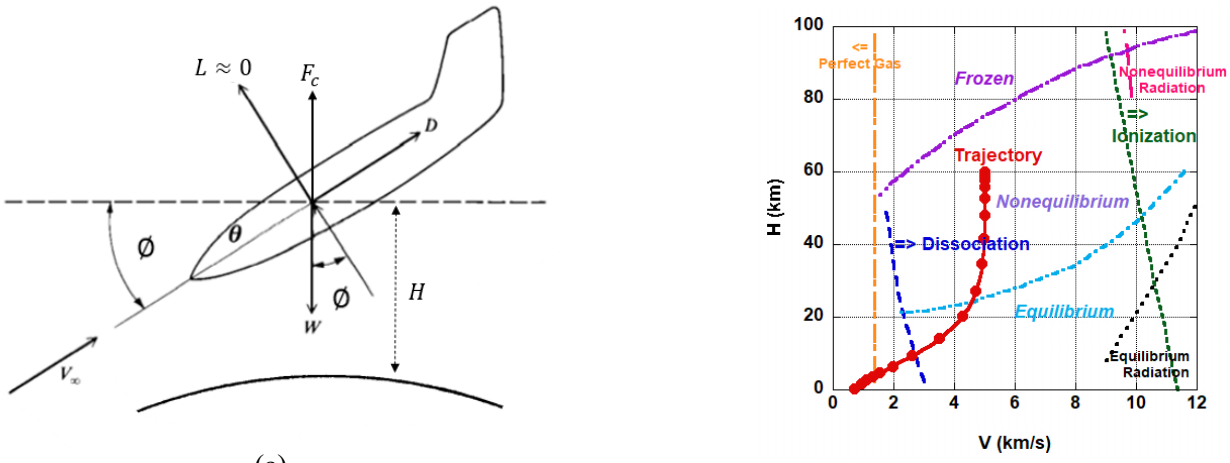

(a) (b)

Fig. 1: (a) Two-dimensional analysis of flight dynamics (b) the velocity-altitude map of hypersonic flight object, juxtaposed with the types of chemical reactions.

Computational Fluid Dynamics

In the investigation of re-entry objects, flight altitudes often extend to several hundred kilometers. However, to maintain the gas in a continuum state, this study adopts a criterion requiring the Knudsen number to be less than 0.001. For objects characterized by a length of 1 meter, the altitude threshold for the continuum flow regime is determined to be 72 km [3]. At altitudes exceeding 60 km, the air density becomes extremely low. Therefore, the study considers the aerodynamic heating effects at altitudes below 60 km by using ANSYS FLUENT software. To streamline the

complexities inherent in the problems studied, several basic assumptions are made: a no-slip boundary condition at the wall and adherence to the ideal gas equation by the gas. The governing equations for hypersonic flow, including the continuity equation (Eq. (5)), the momentum equation (Eq. (6)), and the energy equation (Eq. (7)), are employed in the analysis.

$$\frac{\partial}{\partial t}(\rho) + \frac{\partial}{\partial x_i}(\rho u_i) = 0 \tag{5}$$

$$\rho \frac{\partial}{\partial t}(u_i) + \rho u_j \frac{\partial}{\partial x_j}(u_i) = -\frac{\partial p}{\partial x_i} + \frac{\partial}{\partial x_j}\left[\mu\left(\frac{\partial u_j}{\partial x_i} + \frac{\partial u_i}{\partial x_j}\right)\right] - \frac{\partial}{\partial x_i}\left(\frac{2}{3}\mu \frac{\partial u_j}{\partial x_j}\right) + \rho g_i \tag{6}$$

$$\frac{\partial}{\partial t}(\rho E) + \frac{\partial}{\partial x_i}\left(u_i(\rho E + p)\right) = \frac{\partial}{\partial x_i}\left(k_{eff}\frac{\partial T}{\partial x_i} - \sum_k h_k \vec{J}_{k,i} + u_j \tau_{eff}\right) + S_R \tag{7}$$

where $\rho, u, p, g, E, T, k_{eff}, h_k, \vec{J}_{k,i}, \tau_{eff}$ and S_R is density, velocity, pressure, gravity, energy, temperature, effective conductivity, enthalpy, mass flux, effective shear stress and source term of reaction, respectively.

Nonequilibrium Chemistry

When it comes to the chemical reactions in hypersonic flow fields, it is essential to consider the residence time of the fluid and the characteristic time required for the chemical reactions. While the characteristic time of the reaction is comparable to the residence time, it is known as the chemical non-equilibrium flow. This can be expressed through specific reaction rate equations, such as Finite-Rate Model (Eq.(8)) and modified Arrhenius equations (Eq.(9)). For the non-ionizing air, the common species of hypersonic flow include nitrogen (N_2), oxygen (O_2), nitrogen atom (N), oxygen atom (O), and nitric oxide (NO). The detailed chemical gas reactions [4] considered in the hypersonic flow are listed below including:

$$O_2 \Leftrightarrow 2O\ ; N_2 \Leftrightarrow 2N;\ \ N_2 + N \Leftrightarrow 2N + N;\ NO \Leftrightarrow N + O;\ NO + O \Leftrightarrow O_2 + N\ ;\ N_2 + O \Leftrightarrow NO + N$$

$$\dot{R}_i = \Gamma(v_i'' - v_i')\left(k_f \prod_{i=1}^{n}[C_i]^{\eta_i'} - k_b \prod_{i=1}^{n}[C_i]^{\eta_i''}\right) \tag{8}$$

$$k = AT^{\beta} e^{-\frac{Ea}{RT}} \tag{9}$$

where $\dot{R}_i, \Gamma, v', v'', k, k_f, k_b, C, \eta'$ and η'' is molar rate of reaction, third body efficiency, stoichiometric coefficient for reactant, stoichiometric coefficient for product, reaction constant, forward reaction constant, backward reaction constant, molar concentration, rate exponent for reactant, rate exponent for product, respectively.

Ablation

Carbon-based materials are frequently used as thermal protective material in the nose and leading edges of a hypersonic flight object. This section focuses on the ablative reactions, energy balance, and surface recession. In order to understand the ablation mechanism of carbon-based materials, the study refers to Park's model as the basis for model establishment. The model assumes that recombination of O and N does not occur on the ablative surface. According to experimental results, when C reacts with O and O_2 in high-temperature environments, only CO is detected, and the presence of CO_2 is not observed [5]. Additionally, the primary gas generated during carbon sublimation is C_3 [6]. Combining the above content, the Ablative reactions (Park's model) is listed below, including oxidation, nitridation, and sublimation [7].

$$O + C_{(s)} \rightarrow CO; \quad O_2 + 2C_{(s)} \rightarrow 2CO; \quad N + C_{(s)} \rightarrow CN; \quad 3C_{(s)} \rightarrow C_3$$

Weakly Coupled Analysis with Adaptive Coupling Time Step Approach

The weakly coupled algorithm primarily involves decoupling the entire computational domain into different regions according to their distinct physical properties. Each physical model can use the different time step, in contrast to strong coupling methods where all physical models are required to use the smallest time step. In addition, the coupling time of loosely coupled can be controlled based on the precision of the error, with the chosen objective being to minimize the computational effort within acceptable error margins [8].

Fig. 2 shows the process of weakly coupled method with adaptive coupling time step. Firstly, employing a loosely coupled analysis strategy, the single conjugate heat transfer system is decomposed into two physical models: hypersonic flow field (F) and structural heat transfer (T). Due to the extremely high flow velocities in the hypersonic flow field, a stable state within an extremely short time, the quasi-steady-state results are applied to obtain instantaneous surface heat flux (Q_w) and ablation rates ($\dot{m}_a''$). Through an adaptive coupling time method, the coupling time step sizes for both the flow field (Δt_{fc}) and heat transfer (Δt_{sc}) are calculated, determined by the smaller of the two. The heat conduction and surface recession ($\dot{S}_w$) of solid region is simulated for a period of coupling time. Finally, based on the free-stream conditions of the next trajectory point, the above steps are iteratively performed until the end of the flight time. The values Δt_{fc} and Δt_{sc} are determined by the differences in heat flux and surface temperature integrated over the surface area [9], as shown in Eq.(10)~(11). Additionally, the appropriate time steps are determined based on proportional-integral- derivative (PID) controller [10] (Eq.(12)~(13)). The coupling time step sizes Δt_c is select to be the minimum of Δt_{fc} and Δt_{sc} (Eq.(14)). To prevent the occurrence of overshooting, a maximum value, (Δt_{max}=3s) is assigned if Δt_c is longer than 3s.

$$r_{f_n} = \left(\frac{\int_\Gamma \left(Q_{w_n} - Q_{w_{n-1}} \right)^2 d\Gamma}{\int_\Gamma {Q^2}_{w,n} d\Gamma} \right)^{1/2} \tag{10}$$

$$r_{s_n} = \left(\frac{\int_\Gamma \left(T_{w_n} - T_{w_{n-1}} \right)^2 d\Gamma}{\int_\Gamma {T^2}_{w,n} d\Gamma} \right)^{1/2} \tag{11}$$

$$\Delta t_{fc} = \left(\frac{r_{f_{n-1}}}{r_{f_n}} \right)^{0.075} \left(\frac{1}{r_{f_n}} \right)^{0.175} \left(\frac{r_{f_{n-1}}^2}{r_{f_n} r_{f_{n-2}}} \right)^{0.01} \tag{12}$$

$$\Delta t_{sc} = \left(\frac{r_{s_{n-1}}}{r_{s_n}} \right)^{0.075} \left(\frac{1}{r_{s_n}} \right)^{0.175} \left(\frac{r_{s_{n-1}}^2}{r_{s_n} r_{s_{n-2}}} \right)^{0.01} \tag{13}$$

$$\Delta t_c = min(\Delta t_{fc}, \Delta t_{sc}, \Delta t_{max}) \tag{14}$$

where $r_f, r_s, Q_w, T_w, \Delta t_c, \Delta t_{fc}, \Delta t_{sc}$ and Δt_{max} is the measure of the change of surface heat flux, the measure of the change of wall temperature, wall heat flux, wall temperature, coupling timestep, coupling timestep attribute to r_f, coupling timestep attribute to r_s and threshold of coupling timestep.

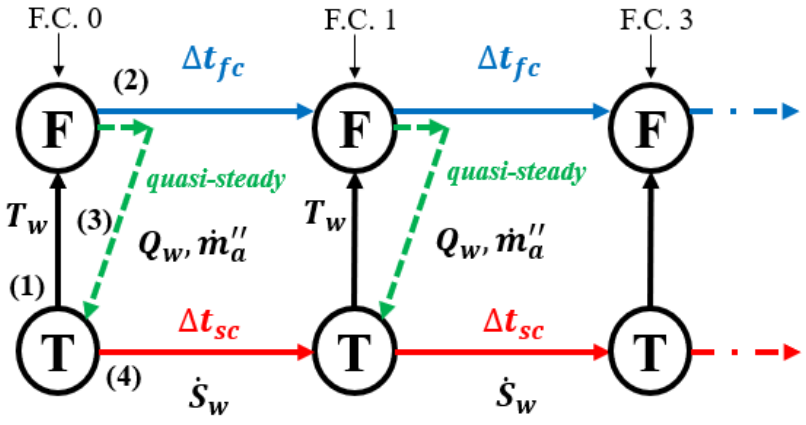

Fig. 2: The flow chart of loosely coupled with adaptive coupling time step.

3. Results and Discussion

The study investigates a hypersonic reentry vehicle (similar to the nose of intercontinental ballistic missile MK 21). Its shape, weight, and ballistic coefficients are presented in Table 1. The research assumes an initial altitude of 60 km and a non-powered descent. Typically, the re-entry velocity of hypersonic flight object at the edge of the atmosphere is about 7 km/s. However, considering the initial altitude within the atmosphere in this study, the re-entry object is inevitably affected by drag. Therefore, the initial velocity is assumed to be 5 km/s. Fig. 1(b) is the velocity-altitude map of hypersonic flight object, juxtaposed with the types of chemical reactions. It can be observed that only dissociation reactions occur during the flight, gradually transitioning from chemical non-equilibrium to chemical equilibrium. The points on the trajectory line represent the separated trajectory points, and their altitude and velocity will serve as the inflow conditions for subsequent simulations.

The study focuses on the analysis of hypersonic thermal loading on the nose region of the hypersonic flight object. Fig. 3(a) shows its computational domain, with the coordinate origin (O). The inlet condition is set as a pressure far-field boundary based on the altitude and velocity at different trajectory points, while the outlet is configured as a pressure outlet. The bottom wall, enveloped within the vehicle, assumes the internal temperature of the vehicle's cabin is consistent with the external ambient temperature (T_∞). Additionally, the temperature on the coupling surface changes according to the results of the fluid-structure coupling. In the numerical simulation, the fluid is represented by a mixture of 77% N_2 and 23% O_2 by mass fraction, replacing actual air. The solid region employs carbon-based material with a density of 1900 kg/m³ and an emissivity of 0.8. The specific heat and the thermal conductivity are varied with the temperature [11].

Table 1: The geometry, weight, and ballistic coefficient of the hypersonic flight object

Based radius	0.55 m
Nose radius	35.56 mm
Length	1.75 m
Half angle	8.2°
Weight	250 kg
Ballistic coefficient	42000 kg/m^2

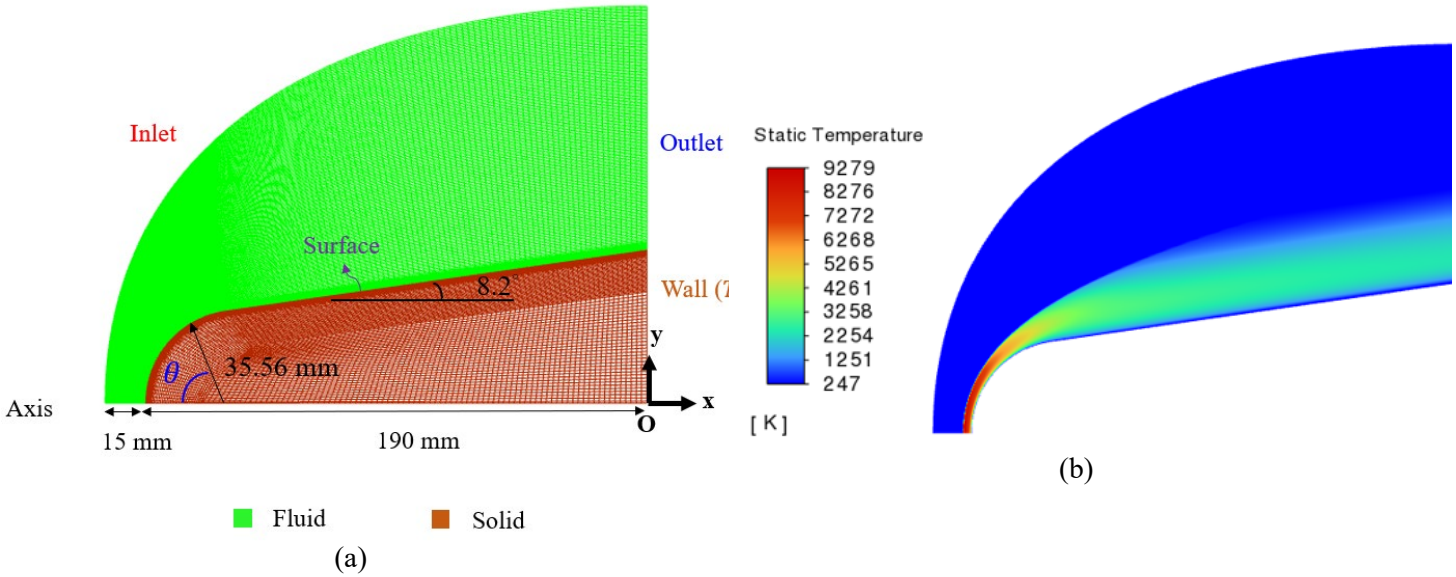

Fig. 3: (a) The computational domain for the nose region of the hypersonic flight object and (b) the contour of temperature in the flow field at t=0s.

The temperature distribution in the flow field at t=0s (initial) is shown in Fig. 3(b). As the fluid passes through the shock wave, the temperature rapidly increases from 247K to over 9000K. This creates a high-temperature gas environment at the front of the object, leading to the dissociation of N_2 and O_2, forming the species N, O, and NO (shown in Fig. 4). Since dissociation is an endothermic reaction, it contributes to reducing the thermal load on the surface.

Fig. 5(a) shows the variation of heat flux at the stagnation point over time. It is evident that the convective heat flux generated by aerodynamic heating remains the primary contribution to surface thermal loading. Since the maximum wall temperature in current study is about 3000K (as shown in Fig. 5(b)), which does not reach the conditions for sublimation (~4000K [6]), the ablation is exothermic reactions of oxidation and nitridation. Additionally, the surface radiation increases as the wall temperature rises. The flight time from t=0s to t=21s corresponds to the aerodynamic heating phase ($Q_{stag.} > 0$), while the flight time from 21 seconds to 35 seconds corresponds to the cooling phase ($Q_{stag.} < 0$). Fig. 5(b) also shows the history of the ablation rate. With the increase in surface temperature and heat flux, there is a noticeable growth in the ablation rate. Simultaneously, the surface mass loss generated by ablation leads to the recession of the surface.

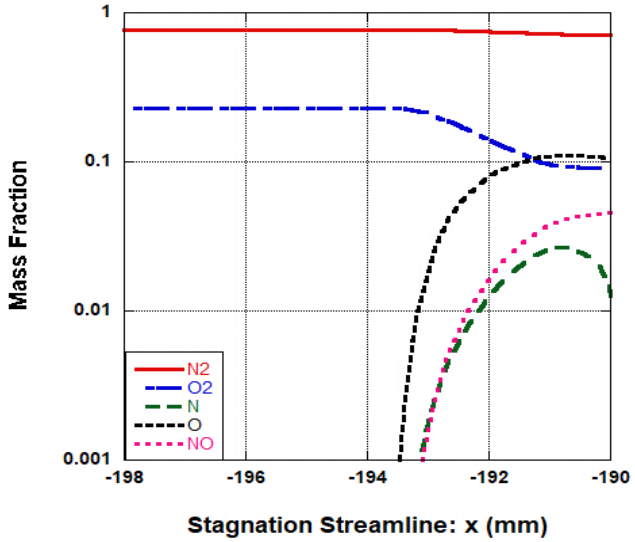

Fig. 4: Mass fraction of various species along the stagnation streamline at t=0s.

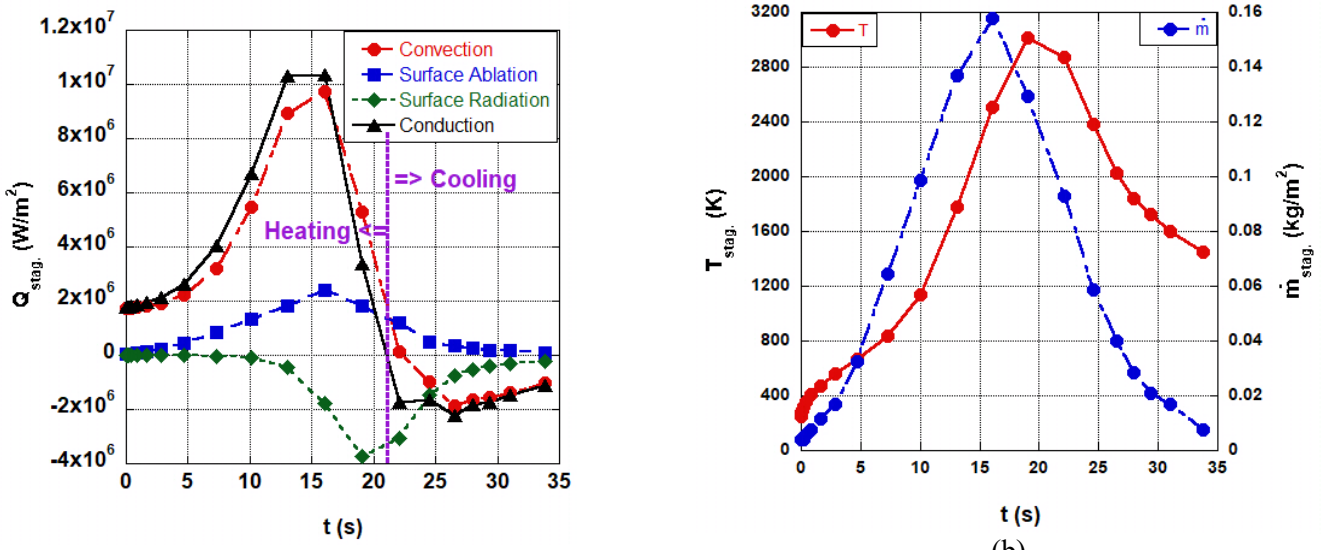

(a) (b)

Fig. 5: The time history of (a) heat flux (b) temperature and ablation rate at the stagnation point.

To obtain the convective heat flux of the stagnation point, $(Q_{conv})_{stag.}$ more efficiently, the study, based on the numerical simulation results (considering the increase in wall temperature), derives the following empirical relationships through analysis using free stream Mach number (M_∞) and pressure (P_∞) as input parameters, as shown in Eq.(15). The constant (C) can be determined by the initial conditions of the flight trajectory. Fig. 6 shows a comparison between Eq.(15) and the numerical simulation results. In addition to the trajectory with an initial speed V_0= 5 km/s as presented in current study, another trajectory with an initial speed V_0=7 km/s was simulated using the same process. The simulation results for both trajectories closely align with the predictions from Eq. (15). Hence, Eq.(15) can be utilized to predict the conjugate heat transfer phenomenon in the hypersonic flow field for carbon-based materials.

$$(Q_{conv})_{stag.} = C\, M_\infty{}^{5.302}\, P_\infty{}^{0.4246} \tag{15}$$

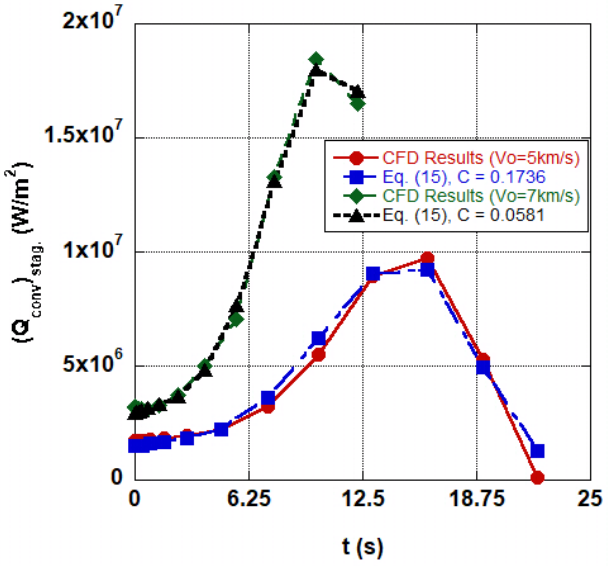

Fig. 6: Comparison of convective heat flux of the stagnation point $(Q_{conv})_{stag.}$ predicted by empirical equation (Eq.(15)) and the numerical simulation results for different initial velocities V_0.

4. Conclusion

This study establishes the re-entry trajectory of an object from attitude 60km. Simultaneously, it employs numerical simulation methods to analyse the thermal loading of the object during its hypersonic flight. The current study adopts a weak coupling approach combined with an adaptive coupling time step method. Compared with the strong coupling method, the adaptive coupling time step method monitors the change of wall heat flux and wall temperature to select an appropriate coupling step size, addressing the uncertainty of coupling time in weakly coupling methods. This approach not only ensures the accuracy of conjugated heat transfer results but also reduces the computational cost from several years to a few days.

During the hypersonic flight, convective heat flux remains the key factor dominating surface thermal loads. Taking the example of the trajectory in this study, the maximum convective heat flux occurs at an altitude of 20 km, reaching 1.03 kW/cm^2, as shown in Fig. 5(a). Moreover, the convective heat flux of the stagnation point can be expressed in terms of the free-stream Mach number and pressure, as shown in Eq.(15). The highest wall temperature reaches 3012 K, as shown in Fig. 5(b).

References

[1] J. M. Eggleston, J. W. Young, "Trajectory Control for Vehicles Entering the Earth's Atmosphere at Small Flight-Path Angles," NASA MEMO 1-19-59L, February 1959.

[2] J. A. White, K. G. Johnson, "Approximate Solutions for Flight-Path Angle of a Reentry Vehicle in the Upper Atmosphere," NASA TN D-2379, July 1964.

[3] T. Rivell, "Notes on Earth Atmosphere Entry for Mars Sample Return Missions," NASA TP-2006-213486, September 2006.

[4] R. N. Gupta, J. M. Yos, R. A. Thompson, "A Review of Reaction Rates and Thermodynamic and Transport Properties for an 11-Species Air Model for Chemical and Thermal Nonequilibrium Calculations to 30000 K," NASA-RP-1232, 1990.

[5] G. Liu, "High Temperature Oxidation of Graphite by a Dissociated Oxygen Beam," Ph.D. Dissertation, Dept. Aeronautics and Astronautics, Massachusetts Institute of Technology, Cambridge, MA, 1973.

[6] J. Abrahamson, "Graphite Sublimation Temperatures, Carbon Arcs and Crystallite Erosion," *Carbon*, vol. 12, no. 2, pp. 111-141, 1974.

[7] Y. K. Chen, F. S. Milos, "Navier–Stokes Solutions with Finite Rate Ablation for Planetary Mission Earth Reentries," *Journal of Spacecraft and Rockets*, vol. 42, no. 6, pp. 961-970, 2005.

[8] K. Gustafsson, M. Lundh, G. Söderlind, "A PI Stepsize Control for the Numerical Solution of Ordinary Differential Equations," *BIT Numerical Mathematics*, vol. 28, no. 2, pp. 270-287, 1988.

[9] S. Zhang, F. Chen, H. Liu, "Time-Adaptive, Loosely Coupled Strategy for Conjugate Heat Transfer Problems in Hypersonic Flows," *Journal of Thermophysics and Heat Transfer*, vol. 28, no. 4, pp. 635-646, 2014.

[10] A. M. P. Valli, G. F. Carey, A. L. G. A. Coutinho, "Control Strategies for Timestep Selection in Finite Element Simulation of Incompressible Flows and Coupled Reaction-Convection-Diffusion Processes," *International Journal for Numerical Methods in Fluids*, vol. 47, no. 3, pp. 201-231, 2005.

[11] R. L. Potts, "Application of Integral Methods to Ablation Charring Erosion, A Review," *Journal of Spacecraft and Rockets*, vol. 32, no. 2, pp. 200-209, 1995.